H. E. Coffey, Ed. (1989), p. 11.
13. *U.S. Standard Atmosphere 1976* (National Oceanic and Atmospheric Administration, Washington, DC, 1976).
14. We thank J. Eisele for his assistance in the early stages of this work. E. Hones and P. Higbie provided insight into the physics of particle storage, loss, and drift in the geomagnetic field. The ephemerides used in these studies were obtained from R. Cote and R. Berry of the Naval Space Surveillance System in Dahlgren, VA. Algorithms for tracing particle trajectories in the geomagnetic field were supplied to us by D. Smart of the Air Force Geophysical Laboratory. We also thank our collaborators E. Rieger, at the Max Planck Institute for Extraterrestrial Research, Garching (Federal Republic of Germany), and E. L. Chupp and D. J. Forrest at the University of New Hampshire for various contributions that they have made to this work. Charged particle data from the Hard X-Ray Burst Spectrometer experiment on SMM were used to confirm the detection of electron events; these data were provided courtesy of B. R. Dennis and his collaborators at NASA Goddard Spaceflight Center.

9 February 1989; accepted 17 March 1989

Distribution and Detection of Positrons from an Orbiting Nuclear Reactor

E. W. Hones and P. R. Higbie

The Solar Maximum Mission (SMM) Gamma-Ray Spectrometer has on many occasions detected nuclear radiation produced by nuclear reactors carried on Soviet satellites. A unique feature of the observations is the measurement of bursts of 511–kiloelectron volt gamma rays that are thought to signal SMM encounters with positrons emanating from the Soviet satellites. A model of positron generation by an orbiting reactor has been developed that describes the resulting time-dependent distribution of positrons temporarily trapped in the geomagnetic field and estimates the response of the SMM spectrometer to passage through such distributions. The model successfully predicts onset times, durations, and intensities of the 511–kiloelectron volt gamma bursts, as we illustrate in a detailed analysis of one event, and thus confirms that these are due to positrons from the Soviet satellites. Reactor-generated positrons are potentially useful in magnetospheric research.

During the past two decades the Soviet Union has placed many nuclear reactor–bearing satellites in low earth orbits, often of ~260-km altitude and 65° inclination (*1–3*). After operating several months they are boosted to ~900-km orbits to delay, for many years, their reentry to the earth's atmosphere. In one case (Cosmos 954) a malfunction caused the reactor to reenter the atmosphere over Canada. Recovery of some of its parts allowed Western scientists to estimate that its operating thermal power level was in the range of tens to hundreds of kilowatts (*1*).

These reactors have constituted unique sources of particles and gamma rays in space. Compton electrons and electron-positron pairs produced near the surface of the satellite by the intense reactor gamma-ray flux can escape. The Solar Maximum Mission (SMM) satellite, launched in early 1980, carried instruments that detected these particles and photons and led investigators to associate them with the Soviet reactor-bearing satellites (*4, 5*). Here we are concerned with the positrons, which are identified by their 511-keV annihilation radiation recorded by a gamma-ray detector on SMM.

Los Alamos National Laboratory, Los Alamos, NM 87545.

The unique properties of positrons as potential tracers for magnetospheric studies were pointed out by Hones (*6*) and hypothetical experiments were described in which reactor-irradiated copper was used as a source of positrons. It is now clear that a nuclear reactor is another potential source of positrons, a fact that, to our knowledge, received no attention prior to the SMM observations described in the accompanying papers.

Positrons emitted nearly perpendicular (90° ± 10°) to the magnetic field by a satellite spiral around the field lines and bounce between their northern and southern mirror points while drifting westward at an angular speed proportional to their kinetic energy. Those outside this range of pitch angles are scattered into the atmosphere and lost at their first or second mirror point because of the low (~260 km) satellite altitude. The geomagnetic field is fairly well described as that of a dipole magnet that is tilted about 11° relative to the earth's rotational axis and displaced about 400 km from the earth's center toward the western Pacific Ocean. This results in there being a region of low field strength over the south Atlantic Ocean, called the South Atlantic anomaly, where drifting particles undergo mirror reflections at lower altitudes than anywhere else and are thus most susceptible to atmospheric loss (*7*).

The expected westward drift of positrons and the expected influences on their lifetimes of the tilt and displacement of the dipole are evident in the distribution, over the earth, of the SMM-Cosmos relative positions during the events. This is illustrated by the following features of Fig. 1 which give qualitative support for the view that the SMM 511-keV gamma events were caused by interception of positrons from Cosmos 1176, temporarily stored in the magnetic field: (i) In all events SMM appears to be closely conjugate to Cosmos or to lie clearly to the magnetic west of it. (Detailed calculations of the satellites' geomagnetic locations show that SMM was at least a degree or so magnetically west of Cosmos in all events.) (ii) Events in the longitude range +150° to −150° (negative means west longitude) all have Cosmos in the northern (magnetic) hemisphere. This is a longitude region

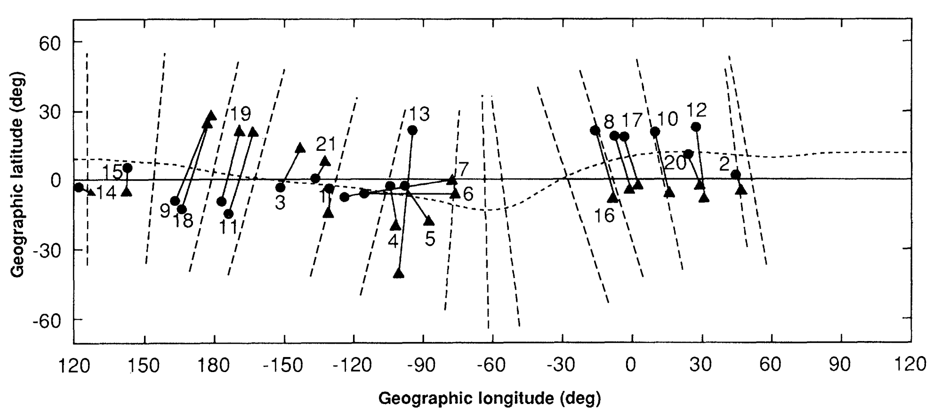

Fig. 1. Locations of SMM (observer) and Cosmos 1176 (source) at the times of 21 of the most intense 511-keV gamma events recorded by SMM during the 29 April to 6 September 1980 operating lifetime of Cosmos 1176. The events are numbered in the chronological order of their occurrence. The coordinates are geographic latitude and longitude. Solid lines join the satellite locations in each event. A dotted line traces the geomagnetic equator. Dashed lines connect magnetically conjugate points on the earth, thus depicting, approximately, magnetic meridians.

where the field is stronger in the southern hemisphere so southern mirror points are higher (by 200 km or so). Positrons emitted nearly perpendicular to the field lines by Cosmos in the northern hemisphere mirror well above the atmosphere in the south and thus can survive one bounce or more. (iii) Events in the longitude range $-20°$ to $+30°$ all have Cosmos in the southern hemisphere. Here the northern mirror points are higher than the southern by several hundred kilometers and arguments analogous to those of (ii) again apply. (iv) Several events, notably 4, 5, 6, and 7, have SMM unusually far to the (magnetic) west of Cosmos. These occurred in the longitude region $-70°$ to $-130°$, on the westward edge of the South Atlantic anomaly, where the field increases westward and mirror points for westward drifting particles rise. The lifetime against atmospheric loss thus increases for the Cosmos positrons as they drift, dramatically increasing the distance over which they can be intercepted by SMM. (v) The two satellites are separated by thousands of kilometers in most events, so some sort of guidance seems required for particles from Cosmos to reach SMM. Theory (*8*) tells us that a charged particle is constrained to move on a magnetic surface defined by two adiabatic invariants of the paticle's motion as it drifts around the earth. Application of this concept to the trapped radiation belts led to introduction of the *L*-parameter to identify a drift surface or "*L*-shell" (*9*). The value of *L* is the equatorial distance, in Earth radii (1 R_E = 6371 km), from the geomagnetic axis to the surface on which a particle is constrained to move. SMM and Cosmos, despite large separation distances, were on closely similar *L*-shells in each event in Fig. 1, supporting the above evidence that SMM was responding to magnetically constrained and guided positrons from Cosmos.

We now present an analysis of event 5 that models the production, injection, loss, drift, and detection of positrons for the event. The final result will be a predicted count rate history for SMM that is then compared with the actual count rate profile measured in the event. Figure 2 illustrates that 511-keV gammas were sensed beginning ~20 s after SMM entered the region of *L*-space that had shortly before been traversed by Cosmos and while the satellites were still 2340 km apart. (Their closest approach occurred 7½ min later.) We shall show that the ~70-s event ended when SMM reached an *L*-shell where the positrons from Cosmos had all drifted past to the west.

To make a quantitative evaluation of this event it was necessary to estimate the following factors: (i) The spectral intensity of positrons released by Cosmos 1176. (ii) The (energy-dependent) lifetime against loss to the atmosphere. (iii) The effect of mirror point rise on atmospheric loss. (iv) Evolution of the longitudinal distribution of positrons. (v) Response of the Gamma-Ray Spectrometer to the spectrum of positrons incident on SMM. The spectral intensity of positrons emanating from Cosmos 1176, shown in Fig. 3, was estimated as described in the figure legend (*10, 11*).

The mean lifetime of positrons against loss by multiple small-angle scattering near their mirror points was calculated by means of methods presented by Christofilos (*12*) and Welch and Whitaker (*13*). The atmospheric model of Kallmann-Bijl *et al.* (*14*) was used for these calculations. It was determined that with parameters appropriate for the orbit of Cosmos 1176 and for the satellite's location in event 5 only about 15% of the positrons would survive the first bounce and the scattering lifetime of the survivors would be $\tau_s \approx 35E^2$ s where E is the positron kinetic energy in megaelectron volts. The surviving percentage of positrons and the lifetime of the survivors are both dramatically increased with decreasing atmospheric density at the altitude of the positron-emitting satellite. This effect is seen in the increasing lifetimes of positrons drifting westward out of the South Atlantic

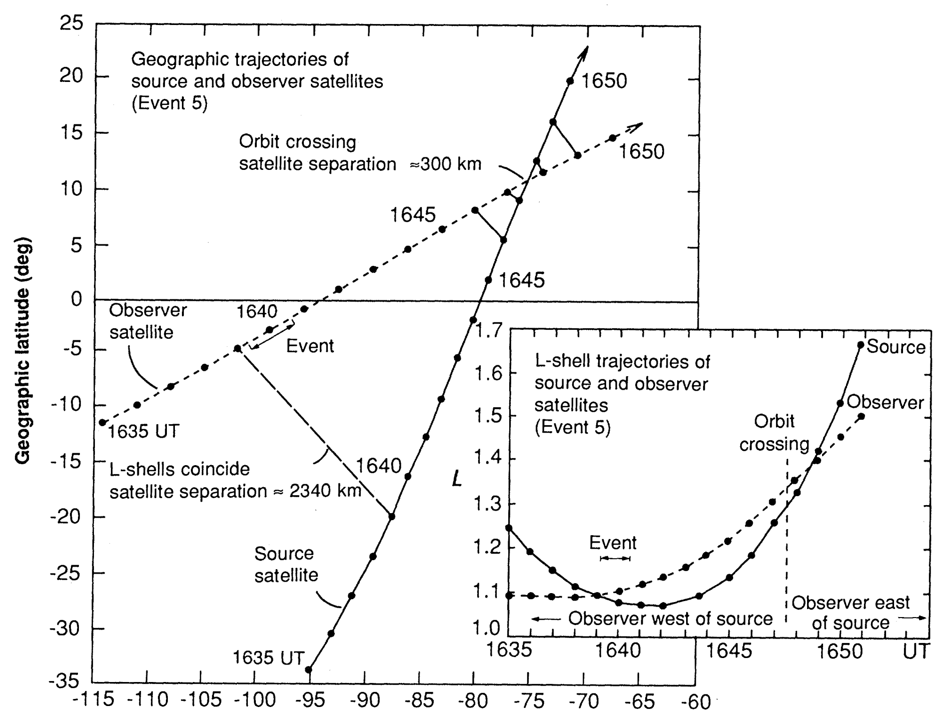

Fig. 2. Trajectories of source satellite (Cosmos 1176 at 263-km altitude) and observer satellite (SMM at 563-km altitude) from 1635 to 1650 UT, 7 May 1980, in geographic latitude and longitude and in *L*-space. "Event" printed by each curve indicates the time interval (16:39:10 UT to 16:40:31 UT) within which 511-keV gammas were sensed by SMM. The peak count rate, corrected for background, was 4.3 counts per second. The closest approach of the two satellites occurred at 16:47:30 when SMM passed eastward 300 km directly above Cosmos.

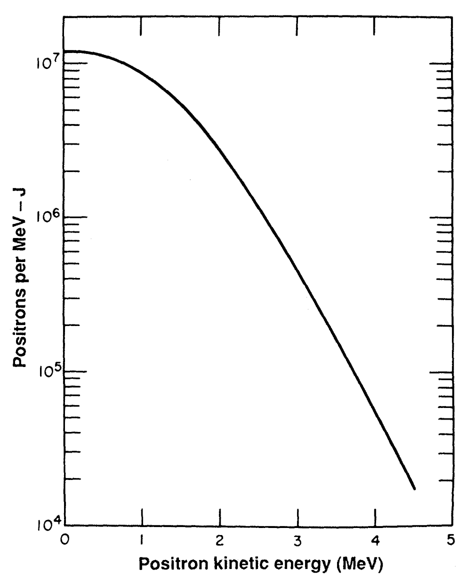

Fig. 3. Estimated differential energy spectrum of positrons escaping from Cosmos 1176. The spectrum of prompt plus delayed gammas from U^{235} fission measured by Maijenschein *et al.* (*10*) was adopted. Formulas and graphs given in Evans (*11*) were used to estimate the spectrum of positrons created in an assumed 1-cm surface layer of aluminum. The spectral intensity of escaping positrons then was calculated from range-energy relations assuming the created positrons were isotropic and of uniform intensity in the aluminum layer.

anomaly (Fig. 1) and in the dependence of the frequency of occurrence of SMM 511-keV gamma events on solar cycle and on Cosmos orbital altitude (5).

The positrons detected by SMM in event 5 were released by Cosmos in a region, on the western edge of the South Altantic anomaly, where the conjugate (northern) mirror point was about 200 km higher than the release mirror point and where mirror altitudes of westward-drifting positrons increased in both hemispheres as shown in world maps of geomagnetic parameters compiled by Wiley and Barish (15). The mirror point rise caused increases in τ_s of the positrons, drifting at angular speed $\omega_d \approx 3.5 \times 10^{-2}\, E/m_0c^2$ degree/s, by factors of ~3 and ~20 for 0.5-MeV and 2.0-MeV positrons, respectively, in the ~100-s duration of event 59 (where m_0c^2 is the positron rest energy).

The positrons that survive injection at a given L form a westward-traveling shell that also expands longitudinally because of the positrons' energy-dependent drift speed. The shell's "thickness" can be thought of as the north-south distance Cosmos moves across field lines in a positron bounce time (~0.1 s), that is, about 1 km. The number of positrons in the energy range δE (MeV) deposited in the shell is the reactor power times the differential emission rate (Fig. 3) times the fraction (~0.15) that survives injection times the shell crossing time. We assumed the reactor thermal power to be 100 kW (1). Figure 4 depicts the evolution of a positron shell estimated for event 5. The principal features are progressive (westward) displacement of the population, longitudinal broadening, and decreasing peak intensity with increasing time.

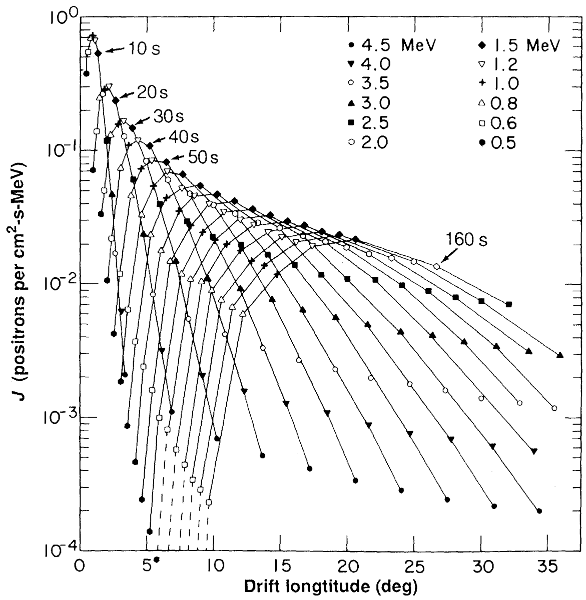

Fig. 4. Distribution of positron flux on an L-shell shown at 10-s intervals after the time of deposition by Cosmos 1176. The abscissa is the geomagnetic longitude measured westward from the longitude of deposition.

Incident positrons are stopped within a few millimeters of the surface of SMM, each creating two 511-keV gamma rays that depart in opposite directions. Those gamma rays that are properly directed to strike the sensitive volume of the gamma-ray spectrometer and are not scattered or absorbed before entering it have a probability of ~80% of being identified as 511-keV gammas and thus signaling the incidence on SMM of their parent positrons. Using simplified models of the satellite and detector to estimate the detector's counting rate in an isotropic flux, J, of positrons, we find that the count rate N (counts per second) $\approx 50\,J$ (positrons cm^{-2} s^{-1}).

We can now present a theoretical interpretation of event 5 for comparison with its observed features. We noted in Fig. 2 that SMM, moving to higher L-shells, first detected 511-keV gamma rays within about 20 s after its L-path intersected that of Cosmos, which was eastward of it, moving to lower L-shells. We can thus visualize SMM, after entering the region of L-space through which Cosmos had just passed, crossing through successive shells of positrons which are in various stages of the evolution depicted in Fig. 4. We note times when Cosmos attained chosen decremental values of L between ~1638 and 1640 UT and then, knowing how much later in time, and how many degrees to the west, SMM crossed the same shells, we determine the positron fluxes at SMM directly from the appropriate curves of Fig. 4.

To illustrate, Cosmos was at $L = 1.113$ at 16:38:00 UT. SMM crossed this L-shell at 16:40:40 UT and did so 11.2° west of the Cosmos crossing. Thus for SMM's crossing of this L-shell we have the parameters $\Delta t = 160$ s and $\Delta\phi = 11.2°$. That is, SMM crossed a 160-s-old positron shell 11.2° west of where it had been established. Entering Fig. 4 we find that the peak flux on the 160-s shell is ~2.2×10^{-2} positrons cm^{-2} s^{-1} MeV^{-1} at drift longitude ≈ 21° (that is, 21° west of where the shell had been established). The flux is only ~1.9×10^{-3} posi-

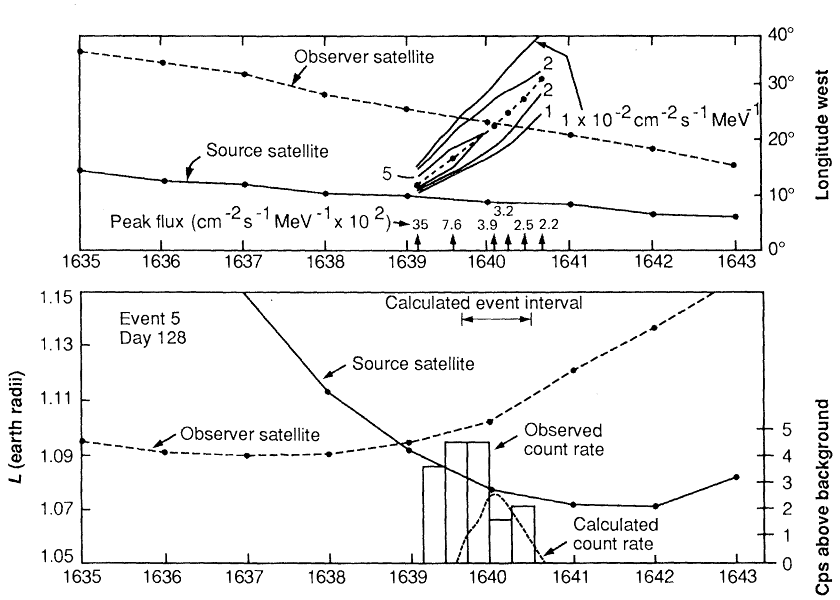

Fig. 5. Analysis of event 5. The trajectories of the source satellite (Cosmos 1176) and the observer satellite (SMM) in L-space are shown in the bottom panel. Their separation in geomagnetic longitude is depicted in the top panel. Isoflux contours of 1, 2, and 5 × 10^{-2} cm^{-2} s^{-1} MeV^{-1} trace the positron distribution on shells of increasing L at the times when SMM passes through them. The calculated event is the time interval (~16:39:40 UT to ~16:40:30 UT) when SMM encounters positron fluxes above its threshold of ~1 × 10^{-2} positrons cm^{-2} s^{-1} MeV^{-1}. The calculated count rate profile during the event is shown as a dashed curve in the bottom panel. The observed count rate profile is shown for comparison.

trons cm^{-2} s^{-1} MeV^{-1}, that is, below the detector threshold ($\sim 1 \times 10^{-2}$), at $\Delta\phi = 11.2°$ where SMM crossed the shell. Flux levels of 1×10^{-2} are found at $\Delta\phi \approx 14°$ and 29° on the 160-s shell; flux levels of 2×10^{-2} are found at $\Delta\phi \approx 28°$ and 22°.

The results of this analysis and comparable analyses of other *L*-shells are shown in the top panel of Fig. 5. For six times from 16:39:08 to 16:40:40 UT the drift longitudes of the peak flux and of flux levels 1, 2, and 5×10^{-2} positrons cm^{-2} s^{-1} MeV^{-1} on the shells being crossed by SMM were determined from Fig. 4. The isoflux contours joining these points, drawn in Fig. 5, trace the evolution, not on a single *L*-shell, but of the positron intensity distributions on successive shells as SMM crossed them. Thus, after ~16:38:50 UT SMM was on shells that contained positrons, but it was not until ~16:39:40 that it encountered a shell on which the positron flux, at the point of crossing, had reached detector threshold levels. The peak flux ($\sim 3.5 \times 10^{-2}$ cm^{-2} s^{-1} MeV^{-1}) was encountered on another shell at ~16:40:04 and after ~16:40:40, SMM was on shells whose positrons had mostly drifted westward of its crossing point.

In the bottom panel of Fig. 5 a dashed curve shows the theoretical count rate profile of the event corresponding to the contour-crossing history in the top panel. Also shown is the observed count rate profile consisting of the five 16.38-s count bins that were above threshold. Our analysis predicts a peak count rate about half that observed, occurring about 20 s after the observed peak time. These differences are easily ascribed to uncertainties in the orbital and physical features of Cosmos as well as to inaccuracies of the model and calculations.

The *L*-shell positions and geomagnetic longitudinal separations of SMM and Cosmos 1176 have been examined for times surrounding all of the events depicted in Fig. 1, although a detailed analysis such as that for event 5 was not done. It was found that the onset times of nearly all the events were consistent with the interception by SMM of ~1- to 5-MeV positrons drifting westward from Cosmos 1176. These many analyses, together with the detailed analysis of event 5 and the qualitative arguments presented earlier with regard to Fig. 1, show that all of the essential features of the SMM 511-keV gamma events can be explained as due to positrons from Cosmos 1176.

REFERENCES AND NOTES

1. *Aviat. Week Space Technol.* (30 January 1978), p. 33.
2. B. M. Jasani, *Outer Space–Battlefield of the Future?*, (Crane, Russak & Co., New York, 1978).
3. *TRW Space Log*, (TRW Space & Technology Group, Redondo Beach, CA, 1978), vol. 23.
4. E. Rieger *et al.*, *Science* **244**, 441 (1989).
5. G. H. Share, J. D. Kurfess, K. W. Marlow, D. C. Messina, *ibid.*, p. 444.
6. E. W. Hones, *J. Geophys. Res.* **69**, 182 (1964).
7. M. Schulz and L. J. Lanzerotti, *Particle Diffusion in the Radiation Belts* (Springer-Verlag, New York, 1974), p. 22.
8. T. G. Northrop and E. Teller, *Phys. Rev.* **117**, 215 (1960).
9. C. E. McIlwain, *J. Geophys. Res.* **66**, 3681 (1961).
10. F. C. Maienschein, R. W. Peele, W. Zober, T. A. Love, in *Proceedings of the Second International United Nations Conference on Peaceful Uses of Atomic Energy* (United Nations, Geneva, 1958), vol. 15, p. 366.
11. R. D. Evans, *The Atomic Nucleus* (McGraw-Hill, New York, 1955), p. 703.
12. N. C. Christofilos, *J. Geophys. Res.* **64**, 869 (1959).
13. J. A. Welch, Jr., and W. A. Whitaker, *ibid.*, p. 909.
14. H. Kallmann-Bijl *et al.*, *COSPAR International Reference Atmosphere 1961* (North-Holland, Amsterdam, 1961).
15. R. E. Wiley and F. D. Barish, *Technical Report no. AFWL-TR-69-114*, (Air Force Weapons Laboratory, Kirtland AFB, NM, 1970).

16. We thank the North American Aerospace Defense Command (NORAD) for providing us the orbital elements for the SMM and Cosmos 1176 satellites. This work was done under the auspices of the U.S. Department of Energy.

2 March 1989; accepted 23 March 1989

Observations of Nuclear Reactors on Satellites with a Balloon-Borne Gamma-Ray Telescope

TERRENCE J. O'NEILL, ALAN D. KERRICK, FARID AIT-OUAMER, O. TUMAY TUMER, ALLEN D. ZYCH, R. STEPHEN WHITE

Gamma rays at energies of 0.3 to 8 megaelectron volts (MeV) were detected on 15 April 1988 from four nuclear-powered satellites including Cosmos 1900 and Cosmos 1932 as they flew over a double Compton gamma-ray telescope. The observations occurred as the telescope, flown from a balloon at an altitude of 35 kilometers from Alice Springs, Australia, searched for celestial gamma-ray sources. The four transient signals were detected in 30 hours of data. Their time profiles show maxima with durations of (21 ± 1) and (27 ± 1) seconds (half-width at half maximum) for the lower two satellites and (85 ± 5) and (113 ± 7) seconds for the remaining two. Their durations place the origin of the two shorter signals at orbital radii of 260^{+40}_{-60} and 260 ± 60 km above the earth and the two longer at 800^{+100}_{-300} and 800^{+250}_{-300} kilometers. Their luminosities for energies >0.3 MeV are then $(6.1 \pm 1.5) \times 10^{15}$, $(3.9 \pm 1.0) \times 10^{15}$, $(1.10 \pm 0.28) \times 10^{16}$, and $(1.30 \pm 0.32) \times 10^{16}$ photons per second. The imaging of the strongest signal indicates a southeastern direction passing nearly overhead. The energy spectrum can be fit to an exponential with index 2.4 ± 1.4. These transient events add to the already large backgrounds for celestial gamma ray sources.

RECENT ARTICLES HAVE DISCUSSED background signals observed by Solar Maximum Mission and Ginga satellite instruments that appear to be caused by nuclear reactors on Soviet satellites (*1, 2*). These signals are produced by electrons and positrons emitted by the hull of the reactor then trapped temporarily in specific regions of the earth's magnetic field. Computer memories of scientific instruments on satellites that fly through these regions are filled, preventing the detection of celestial radiation. Suggestions have been made to shut down instruments on NASA's Gamma Ray Observatory (GRO), which will be launched into earth orbit in the near future, as it passes through these regions or to disregard the radiation when simultaneously detecting electrons or positrons. Direct gamma-ray emission may also cause a significant increase in the background radiation.

Department of Physics and Institute of Geophysics and Planetary Physics, University of California, Riverside, CA 92521.

Here we report the detection of direct gamma-ray emission from four different satellite reactors. The observations were made during a 30-hour period with the University of California, Riverside (UCR), double Compton telescope launched from a balloon to an altitude of 35 km. We observed two satellites at 260-km altitude and two at 800 km, the latter above the future orbit of GRO. The flux we detected from the nearest reactor exceeded by 50 times the flux expected from the strongest celestial sources. The Comptel experiment on GRO, which is similar to our instrument and which possesses a large field of view and high sensitivity, could also be subjected to these enormous signals (*3*).

The UCR double Compton telescope (*4, 5*) was designed to search for celestial gamma-ray sources at energies of 1 to 30 MeV. Because the aperture of the instrument is about 1 steradian, virtually the entire southern sky could be searched in 24 hours from Alice Springs, Australia.